International Journal of Engineering Research and Technology. ISSN 0974-3154, Volume 12, Number 9 (2019), pp. 1598-1604


# Pollen Grain Recognition Using In-focus Surface and Sequence Alignment

**Sultan M. Almotairi***

*Department of Natural and Applied Sciences, Community College,*
*Majmaah University, Al- Majmaah 11952, Saudi Arabia.*
*ORCID: 0000-0003-2050-5236*

**Abstract**

Pollen analysis and identification is widely used in palaeoenvironmental reconstruction, palynonlgy research, and medical studies. The process of classifying pollen grains is a time consuming task even for experienced experts. Therefore, computerizing this routine using computer vision techniques is highly needed. Despite recent advances in computing and texture analysis, automatic pollen classification still remain unsolved. In this paper, we present a method for classifying pollen grain obtained from an optical-microscopy. Each pollen grain is represented by sequence of images taken from different depth using multifocal microscopy. First, we segment the background and pollen by the means of the in-focus areas from each slice. Secondly, the surface textures of pollens are extracted from the in-focus areas. Finally, when approaching this problems, we use sequence alignment to match between the learned model and a new data. Even though our method developed for pollen identification, it is applicable for other microscopy objects classification. Experiments performed on tropical fossil pollen dataset acquired using optical microscopy.

**Keywords:** Pollen recognition; Visual Texture; Sequence Alignment; Longest Common Subsequence; RPCA

## 1. INTRODUCTION

The classification required analyzing the pollen's surface texture by identifying its geometrical features (e.g., ridges and spikes) and the presence of prose. Here, we present a novel method for pollen classification. The method uses multifocal image sequences obtained using optical microscopy. In Fig. 1., a graphical overview of our method is shown. It consists of four steps. At first, we use the Robust Principal Component Analysis (RPCA) [1] to extract a pollen contour regions from each image in the sequence. This step discard unwanted neighboring information such as debris and background. Once the pollen has been extracted, we use exposure fusion [2] to extracted in-focus areas. These areas are the best exposed and/or the best focused regions of the pollen surface. Then, we describe the texture appearance of these regions using Segmentation based Fractal Texture Analysis (SFTA) [3]. The computed features encode information for each slice about the orientation and scale of pollen surface features. The identification of a given pollen is done by performing matching sequence of feature vectors using powerful sequence alignment methods (i.e., Longest Common Subsequence (LCSS)[4]). Finally, recognition of a pollen is done using k-nearest neighbors algorithm (KNN) [5] based on matching scores obtained from LCSS. As shown in the experiments section, the method performs well for tropical fossil pollen identification.

## 2. RELATED LITERATURE

The research of pollen grain identification is quite limited. However, recent research shows that it is possible to classify pollen grains based on visual texture [6, 7, 8, 9, 10], contour [11, 12, 13], and 3D shape [14]. Carrión et al. [7] classified honeybee pollens based on texture image classification generated using a multiscale filtering scheme. Whereas, Guru et al. [6] used Local Binary Pattern features to describe surface textures. Ticay-Rivas et al. [10] and by Rodriguez-Damian et al. [15] encoded brightness descriptors derived from pollen intensity images. However, these descriptors cannot capture the small details of a pollen grain surface. Also, many pollen grain cannot be solely distinguished by their color measurement.

Some recent methods classify the pollen using the shape of the outer contour [11, 12, 13]. Ranzato et al. [11] developed a method to classify pollen that can deal with variability within each class based on the interest points on the outer contour. These features are invariant with respect to rotation, shift, and scale. Similar approach by Travieso et al. [12] proposed the use of morphological details of the contour by combining statistical reasoning, feature learning. Also, Rodriguez-Damian et al., [13] classifies pollen based on their morphology (outer-contour) and their sculpture (texture of the inner grain) based on 2D images. However, to identify pollen correctly more than one image at different focus may be needed.

Finally, Ronneberger et al. [14] obtained 3D volume data for each pollen grain with a fluorescence microscope. They used a support vector machine to classify the extracted features that are 3D invariant. In contrast to their approach, our method works on a dataset obtained from an optical-microscopy without using expansive tools such as the fluorescence microscope, even though we were able to achieve a good accuracy result.

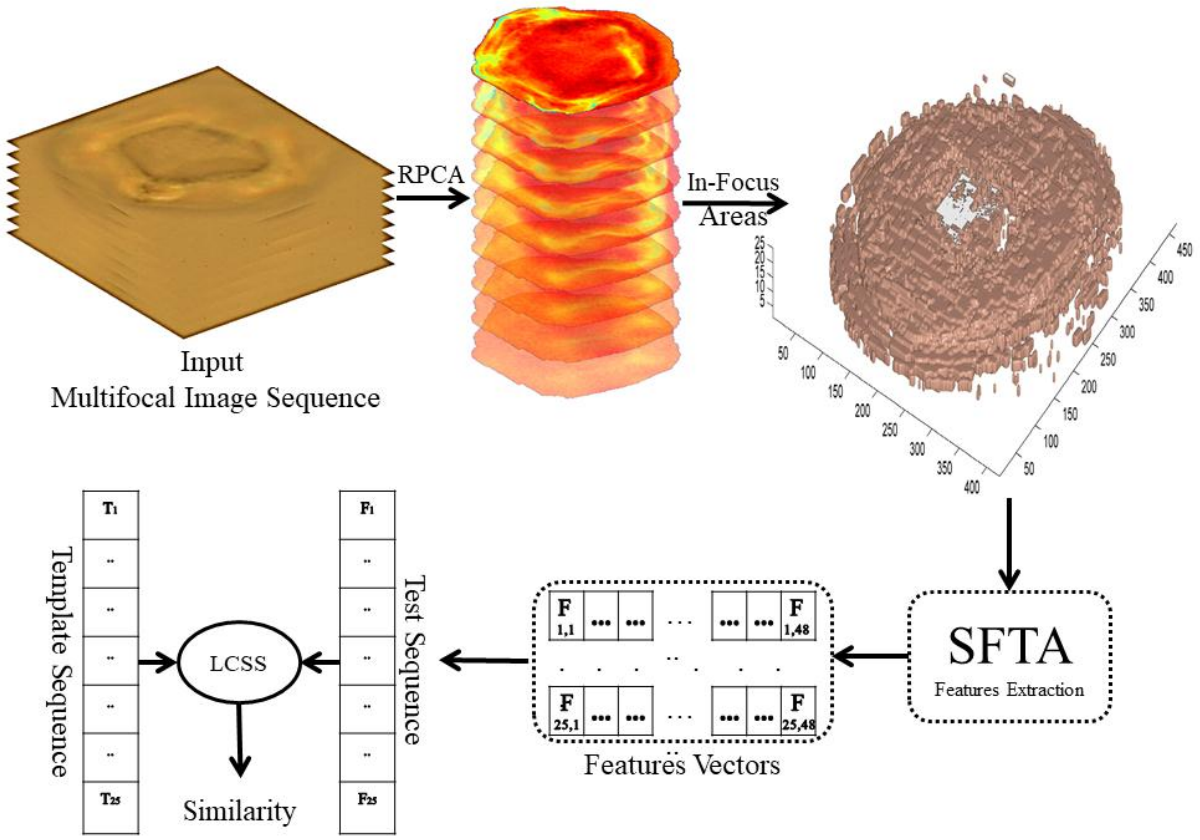


**Fig. 1.** Overview of our method. First, a multifocal image sequence is given as input. Second, background removed and Pollen region extracted using RPCA. Then, in-focus areas are extracted from the whole sequence using exposure fusion. For each slice, the appearance features is computed using SFTA. Finally, LCSS algorithm were used to compare the final features vector to the training database.

Shafaey et. al. [19] [20] used conventional image processing techniques to segment and classify biological particles in microscopic images. The method is based on maximizing the contrast between the particles and liquid environment then the particles are segmented using Otsu thresholding or Watershed transform. The particles are then classified using size, shape and texture features. The proposed method allows for algae particles to be correctly identified with accuracies up to 99%.

Different segmentation and processing techniques for medical and bioimages are presented in [17][18]. The segmentation techniques are categorized as Statistical, Template, Edge, and Region-based techniques.

## 3. PROPOSED METHOD

### 3.1 Data Pre-processing

The First step is detecting the pollen grain on each multifocal image sequence (see Fig. 2., top row is the raw images). Extracting the pollen from its sequence is challenging task due to undefined and blurred pollen's boundaries. Also, the foreground and background image regions could have very similar intensity and color. Moreover, debris might be present in the sequence.

We overcome these challenges by accumulating and using information from all images in the sequence and then use it to improve the detection of the pollen grains. To achieve this goal, we begin by using the Robust Principal Component Analysis (RPCA) [1] to remove the static background. This is accomplished by assuming that the change in-focus between each level in the multifocal sequence occurs only on pollen's contour.

### 3.2 Background Modeling

We begin by describing the Robust Principal Component Analysis [1] for the segmentation of pollen from multifocal image sequence. Let assume that $S = (S_1,...,S_n)$ be a sequence of multifocal images of a specific pollen grain using measurements of the optical-microscopy at n consecutive depths, where $S_1$ is acquired at the highest depth and Sn is at the lowest depth. If slice frames for each multifocal sequence are stacked as columns of a matrix D, then matrix can be written as the sum of a sparse error matrix and a low-rank background matrix representing the change in the scene (i.e., change in pollen surface). If there is no significant change in illumination on the frame background, but most of changes occurs on the pollen surface, then RPCA is very effective in separating the

background from the image. The main idea is decompose the observed data matrix D ∈ $R^{m\times n}$ into low-rank matrix A and sparse error matrix E. So, the Lagrangian reformulation of this optimization problem is shown in Eq. 1. Where D is the observed data matrix $D \in R^{m\times n}$ and $n$ is the number of slice and the $m$ is individual frames are stacked as columns, and $\lambda$ is a parameter that controls the trade-off between sparsity and the rank of $L$.

$$\min_{A,E} \ \text{rank}(A) + \lambda\left|\left|E\right|\right|_0 \ \ \text{subj.to} \ \ \text{A} + \text{E} = \text{D}, \quad (1)$$

However, Eq. 1. is a non-convex optimization problem. Therefore, it can be relaxed to obtain tractable optimization problem, by replacing the λ0−norm with λ1−norm and the rank with the nuclear norm, resulting the following convex surrogate:

$$\min_{A,E} \ \left|\left|A\right|\right|_* + \lambda\left|\left|E\right|\right|_1 \ subj.to \ \ A + E = D, \quad (2)$$

Prior to performing the texture analysis, we prepossess all sequences using this technique. This pre-processing step helps reduce noise and remove the background, while preserving the geometrical details of pollen's surface. However, in our algorithm all multifocal sequences were converted to gray-level to perform RPCA.

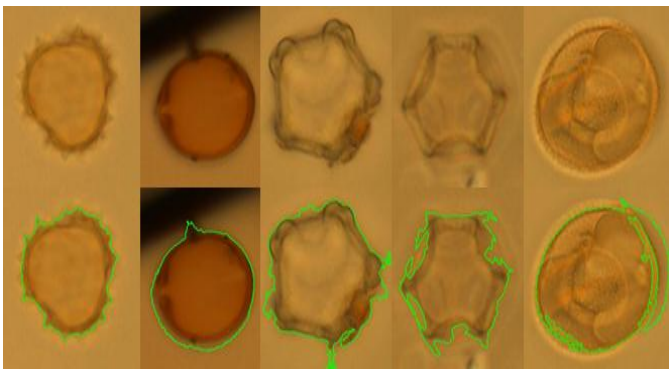

**Fig. 2.** Segmentation examples for multifocal sequence on different pollen grain. Noise and background in the examples are largely reduced while boundary of pollen is preserved. With the segmented multifocal slices of pollen at hand, we can extract the in-focus surface from each slice.

### 3.3 Multifocal exposure fusion

The basic idea is that pixels in the input multifocal sequence images are weighted according to qualities. There are three diffident weight were used, namely, proper exposure, good contrast, and high saturation. However, these criteria used to determine how much each pixel from a slice can contribute to the final slice. The proper exposure criteria favors pixels with luminance, whereas saturation and contrast favors highly-saturated and high contrast pixels, respectively. We use exposure fusion [2, 16] approach often applied in merging overlapping images. The exposure fusion framework presented in [2] is more applicable to the extraction of in-focus pixels on each slice as it accounts for saturation and contrast. Fig. 3. shows an example of infused multifocal sequence imaging [2]. However, we used this technique not to merge the entire sequence into one image, but to detect the in-focus pixels on each slice.

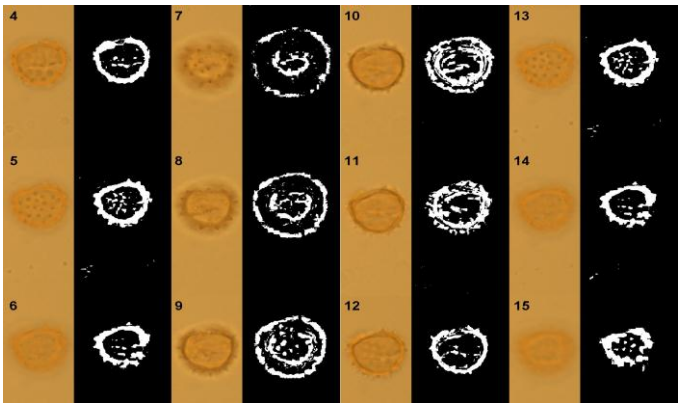


**Fig. 3.** Samples of segmentation of pollen grain. A single image at depth 12 of the segmented multifocal sequence is shown. The segmentation is performed on the whole sequence. The first row shows the original image and the second row show the segmented pollen using RPCA.

We start by defining the (quality weight measures) by describing the exposure fusion proposed by Mertens et al. [2] for the extraction if an in-focus surface pixels from each slice. For each pixel, we combine the information from the measurements of contrast, saturation, and well-exposedness into a scalar weight map from all the slices. The influence of all measurement is given by:

$$W_{ij,k} = \left(W_{ij,k}\right)^{\omega\text{C}} \times \left(W_{ij,k}\right)^{\omega\text{S}} \times \left(W_{ij,k}\right)^{\omega\text{E}} \quad (3)$$

where C, S, and E represent contrast, saturation, and well-exposedness, respectively. Whereas, ωC, ωS, and ωE their corresponding weight. The measurement of contrast done by applying Laplacian filter (e.g., [0 1 0; 1 -4 1; 0 1 0]) to the gray-scale version of each slice and then take the absolute value of the result. The measurement of saturation is calculated as the standard deviation of the color channels, whereas well-exposedness is computed by the mean of how well a pixel is exposed by keeping the small intensity (close to zero) and big intensity (close to 1). Each intensity $i$ is weighted based on how close it is to 0.5 using a Gaussian curve on each slice separately:

$$\exp\left(-\frac{(i-0.5)^2}{2\sigma^2}\right), \qquad where \qquad \sigma = 0.2$$

To obtain a consistent result, each values of $N$ weight maps at each pixel $(i,j)$ is normalized such as they sum to one as follows:

$$\widehat{W_{ij,k}} = \left[\sum_{\acute{K}=1}^{N} W_{ij,\acute{K}}\right]^{-1} W_{ij,k} \quad (4)$$

Finally, the resulting fused image and the in-focus masks can be then obtained by blending of the multifocal sequence images:

$$L\{R\}_{ij}^{l} = \sum_{K=1}^{N} G\{\widehat{W}\}_{ij,k}^{l} L\{I\}_{ij,k}^{l} \quad (5)$$

where ℓ is the level of resulting Laplacian pyramid and $L\{R\}^{\ell}$ contains the mask that used to extract the in-focus surface form

each slice. However, the final fused image can be obtained by collapsing $L\{R\}^{\ell}$.

### 3.4 Modeling the texture

The pollen surface provides very descriptive features (e.g., granularity and repetitive patterns) of what is the type of pollen. These features include symmetric placement of blob-shaped regions and elongated shapes which appear at variance scale and orientations. However, the shape and surface features of pollen multifocal sequence are chaining on each slice (e.g., different depth), which our method takes advantage of it by matching and comparing individual slices. Here, we represent each image as a vector *F* extracted from the input gray-scale image using Segmentation-based Fractal Texture Analysis (SFTA) algorithm [3].

The SFTA extraction algorithm starts by decomposing the input slice into a set of binary images using Two-Threshold Binary Decomposition (TTBD) algorithm. Then, a fractal dimensions of each regions are calculated in order to describe segmented texture patterns.

Each image from the multifocal sequence obtained from the previous section which contains only the areas in-focus is converted to gray-scale image. Then, TTBD were applied to decompose the slice into a set of binary images $n_t$ as follows:

$$\mathrm{I}(x,y) = \begin{cases} 1 & if\ t\omega \le I(x,y) \le t\mu \\ 0 & otherwise. \end{cases} \quad (6)$$

where $t\omega$ denote lower threshold and $t\mu$ denote upper threshold (i.e., $t\omega$ and $t\mu \subset$ T ). Fig. 4. illustrates the decomposition of a region taken from a pollen multifocal sequence at depth 12.

Finally, the SFTA feature vector is constructed for each slice as follows:

$$\Delta(\mathrm{x,y}) = \begin{cases} 1 & if\ \exists(x',y') \in N8[(x,y)]: \\ & I_b(x',y') = 0 \wedge \\ & I_b(x,y) = 1 \\ 0 & otherwise. \end{cases} \quad (7)$$

where $N8[(x,y)]$ is the set of pixels that are 8-connected to $(x,y)$. Fig. 4. shows an overview of SFTA algorithm used to extract feature on each slice (For more details on SFTA implementation please refer to [3]). However, the time complexity to extract the features for each multifocal sequence is $O(S \times N \times T)$, where *S* is the number of slices, *N* number of pixel on each slice, and *T* is the number of thresholds obtained by multi-level Otsu algorithm [21].

### 3.5 Identification using sequence matching

In this section, we perform classification by means of the similarity measurement between multifocal sequence by giving more weight to the similar portions of the sequence using LCSS[4]. However, the identification was done by means of the nearest-neighbor classification scheme based LCSS.

The matching process of multifocal sequence and calculating the similarity between two sequence done as follow. Given a sequence $S_1$ and $S_2$ of lengths $s_1$ and $s_2$, respectively, then the sequence alignment function is given by:

$$\mathrm{LCSS(i,j)} = \begin{cases} 0 & i = 0, \\ 0 & j = 0, \\ LCCS(i-1,j-1)+1 & if\ D(i,j) \le \epsilon, \\ Max[LCSS(i,j-1), LCSS(i-1,j)] & D(i,j) > \epsilon, \end{cases} \quad (8)$$

where $1 \le j \le s_2$ *and* $1 \le i \le s_1$ *and D(i, j)* contains the distance between slices (i.e., a feature vector using SFTA) *i* and *j* as calculated using Eq. 9.

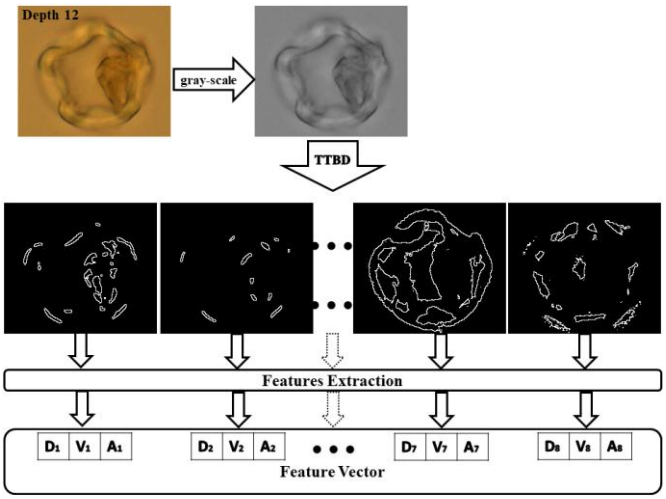


**Fig. 4.** Steps for features extraction using SFTA. Demonstration of the TTBD decomposition step performed on original slice of Alnus pollen at depth 12 and $n_t$ =8. Then, fractal measurements is computed for each region (i.e., A,V,D denote area, mean, and fractal dimension, respectively.). Actual SFTA algorithm is performed on the entire sequence obtained.

$$\mathrm{D}(F_i, F_j) = \chi^2\left((F_i, F_j)\right) \quad (9)$$

where *Fi, Fj* is the feature vector calculated by SFTA for *i* and *j* slice, respectively. The $\chi^2$ is the chi-square histogram distance [22]. However, extracting the cost of matching sequence $S_1$ to $S_2$ is accomplished as follows:

$$\mathrm{Cost}(\epsilon,\delta,\mathrm{S_1},\mathrm{S_2}) = 1 - \frac{\max\left(\mathrm{LCSS}_{\epsilon,\delta}(\mathrm{S_1},\mathrm{S_2})\right)}{\min(\mathrm{s_1},\mathrm{s_2})} \quad (10)$$

Algorithm 1. summarizes the main steps of our method. Finally, recognition of a pollen is accomplished by means of a nearest-neighbor classification scheme based on LCSS.

## 4. EXPERIMENT RESULTS

We evaluate the effectiveness of proposed method. We use a set of multifocal sequences of pollen grain acquired at Paleoecology Laboratory [23] using Zeiss Axioscop equipped with a motorized Ludl stage. This dataset contains multifocal sequence for the Waltheria, Alternanthera, Scalesia, Darwiniothamnus, and Alnus pollen. Each sequence were obtained using 25 consecutive focal length. In our experiments,

sub-regions containing the pollen were manual selected. Fig. 5. shows samples of multifocal sequence images for each type of pollen from the used dataset.

Algorithm 1. Features extraction and alignment

Input: $A$ and $B$ are two multifocal sequences

Output: similarity measurement between them

1. $a \leftarrow$ number of slice in the sequence $A$
2. $b \leftarrow$ number of slice in the sequence $B$

   //in our experiments a ≡ b=25
3. $A_a$, $B_b$ $\leftarrow$ remove background using RPCA (Eq. 2)
4. $W_a$, $V_b \leftarrow$ obtain in-focus surfaces using Exposure-Fusion for both sequences $A$ and $B$, respectively. (Eq. 5)
5. for $i \leftarrow 1$ to $a$ do

   $F_{a_i}$ = Feature vector using *SFTA* ($W_{a,i}$) $\leftarrow$ (Eq. 7)

   $F_{a_i}$ = Feature vector using *SFTA* ($F_{b,i}$)
6. Obtain matching cost between $F_a$ and $F_b$ using LCSS (Eq. 8)
7. compute the similarity using (Eq. 10)
8. return *the similarity between A and B*

   //range from 0 to 1, smaller value means more similarity

We extracted the in-focus areas extracted from the multifocal sequences using other methods such as Frequency-tuned (FT) salient region detection [24] and Spatiotemporal Saliency Map (SSM) [24]. The Fig. 6. shows that FT and SSM work well when the slice contains height contrast, but fails when the slice mostly out-offocus. The hard mask avoids averaging of fine details at the expense of increasing the noise (i.e., improves the sharpness), whereas the normal mask that used in our method created using the original exposure fusion [2] without constrains.

In Fig. 7., we presented the classification result using confusion matrix (82.8% recognition rate). Also, we can see that the most confusion occurred between Alnus, Darwiniothamnus, and Alternanthera grains due to the similarity in outer boundary of the pollen. Also, this confusion occurred due to the absent of the internal geometer on most of the slices (mostly visible on the 5 middle slices). This can be solve by increasing the weight of the matching middle slices an less white for the margins. However, overall our method was able to achieve a comparable result to the visual inspection.

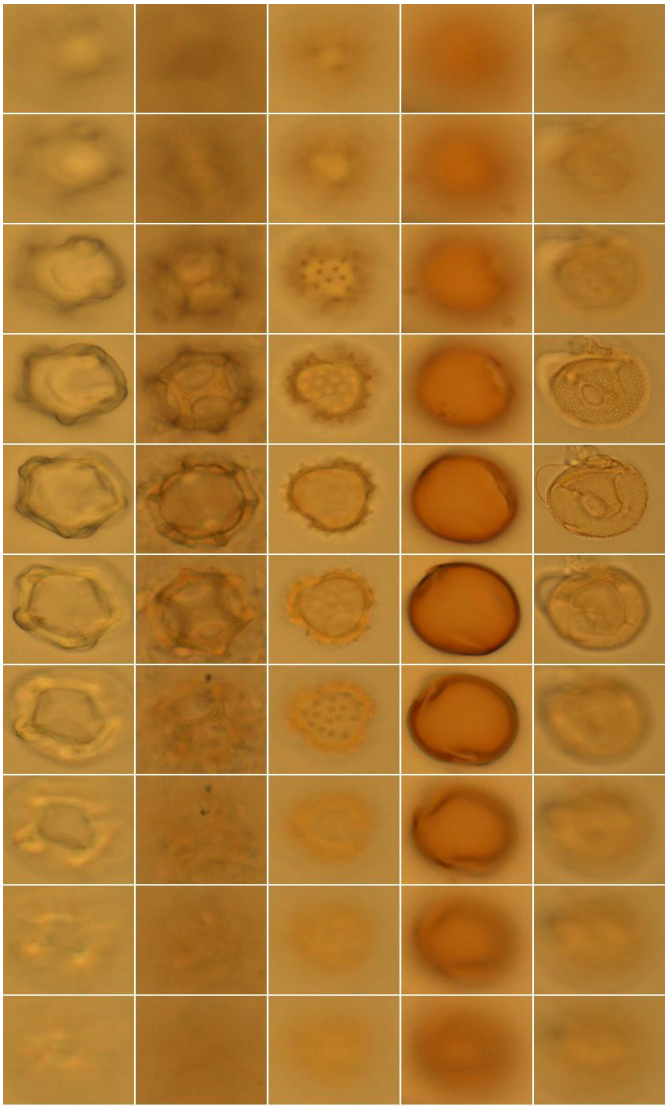

**Fig. 5.** Samples of multifocal sequence images for different types of pollen grains. These are tropical fossil pollen (Alnus, Alternanthera, Darwiniothamnus, Scalesia, and Waltheria) acquired at Paleoecology Laboratory [23] using optical microscopy. The demonstrated slices acquired from depth 4 to 22, using every other slice.

## 5. CONCLUSIONS

We proposed a working prototype of a system to classify pollen obtained from multifocal image sequence. We used RPCA to extract the pollen grain regions. Then, we used exposure fusion to identify in-focus areas. These areas are the best exposed and/or the best focused regions of the pollen surface. Then, we described the texture appearance of these regions using SFTA. Finally, the identification was performed by matching sequence of feature vectors using LCSS. Recognition was done using k-nearest neighbors algorithm based on LCSS. The main novelty of our approach lies in addressing the in-focus areas and then use sequence alignment to classify pollen.

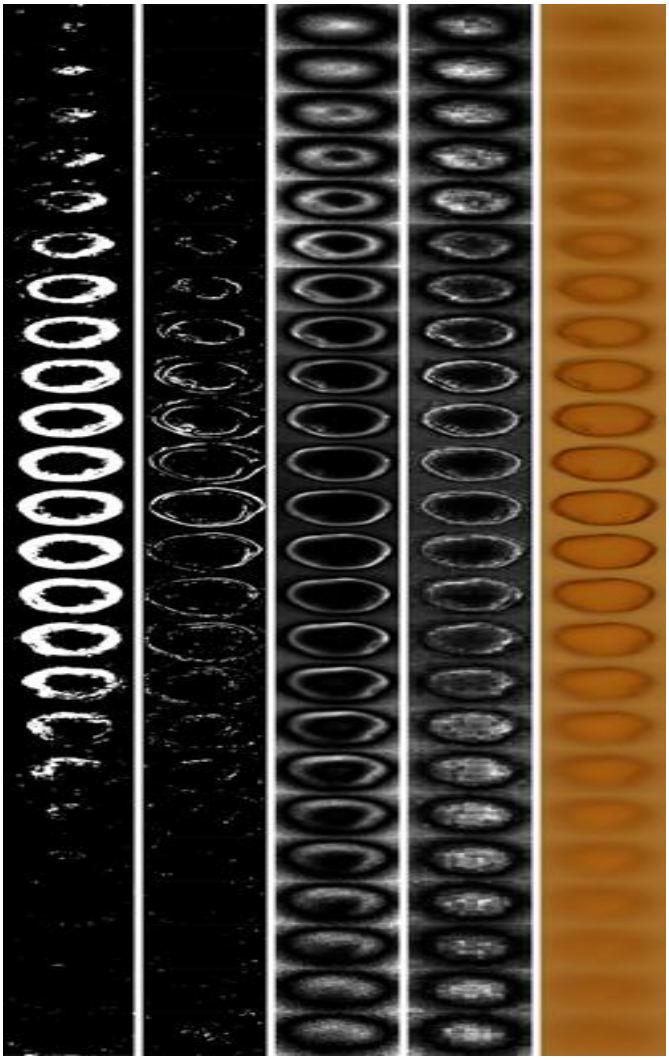

**Fig. 6.** Given input images (right), (2nd column) Frequency-tuned (FT) salient region, (3rd column) Spatiotemporal Saliency Map (SSM).

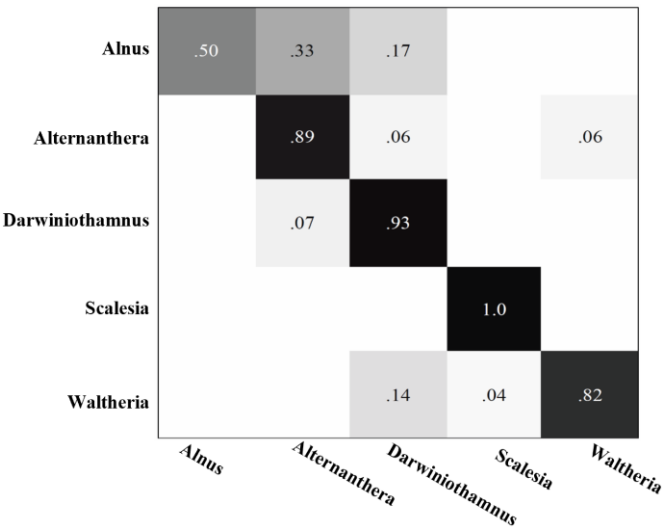


**Fig. 7.** The confusion matrix of our approach on the tropical fossil pollen dataset. Our method accomplished 82.8% recognition rate.

## REFERENCES

[1] J. Wright, "Robust principal component analysis: Exact recovery of corrupted low-rank matrices via convex optimization," in Advances in Neural Information Processing Systems, 2009.

[2] T. Mertens, J. Kautz, and F. Van Reeth, "Exposure fusion," in Pacific Conference on Computer Graphics and Applications, Oct 2007, pp. 382–390.

[3] A. Costa, G. Humpire-Mamani, and A. J. M. Traina, "An efficient algorithm for fractal analysis of textures," in 25th Conference on graphics, patterns, and images (SIBGRAPI), Aug 2012, pp. 39–46.

[4] M. Vlachos, G. Kollios, and D. Gunopulos, "Discovering similar multidimensional trajectories," in Proceedings of 18th International Conference on Data Engineering, 2002, pp. 673–684.

[5] N. Altman, "An introduction to kernel and nearestneighbor nonparametric regression," American Statistician - AMER STATIST, vol. 46, pp. 175–185, 1992.

[6] D. Guru, S. Siddesha, and S. Manjunath, "Texture in classification of pollen grain images," in Multimedia Processing, Communication and Computing Applications, ser. Lecture Notes in Electrical Engineering, P. P. Swamy and D. S. Guru, Eds. Springer India, 2013, vol. 213, pp. 77–89.

[7] P. Carrión, E. Cernadas, J. Gálvez, M. Damián, and P. Sá-Otero, "Classification of honeybee pollen using a multiscale texture filtering scheme," Machine Vision and Applications, vol. 15, no. 4, pp. 186–193, 2004.

[8] P. LI, W. J. Treloar, J. R. Flenley, and L. Empson, "Towards automation of palynology 2: the use of texture measures and neural network analysis for automated identification of optical images of pollen grains," Journal of Quaternary Science, vol. 19, no. 8, pp. 755–762, 2004.

[9] Y. Zhang, D. W. Fountain, R. M. Hodgson, J. R. Flenley, and S. Gunetileke, "Towards automation of palynology 3: pollen pattern recognition using gabor transforms and digital moments," Journal of Quaternary Science, vol. 19, no. 8, pp. 763–768, 2004.

[10] J. Ticay-Rivas, M. Pozo-Baños, C. Travieso, J. Arroyo-Hernández, S. Pérez, J. Alonso, and F. Mora-Mora, "Pollen classification based on geometrical, escriptors and colour features using decorrelation stretching method," in Artificial Intelligence Applications and Innovations, ser. IFIP Advances in nformation and Communication Technology, L. Iliadis, I. Maglogiannis, and H. Papadopoulos, Eds. Springer Berlin Heidelberg, 2011, vol. 364, pp. 342–349.

[11] M. Ranzato, P. E. Taylor, J. M. House, R. C. Flagan, Y. LeCun, and P. Perona, "Automatic recognition of biological particles in microscopic images," Pattern Recogn. Lett., vol. 28, no. 1, pp. 31–39, Jan. 2007.

[12] C. Travieso, J. Briceno, J. Ticay-Rivas, and J. Alonso, "Pollen classification based on contour features," in IEEE International Conference on Intelligent Engineering Systems, June 2011, pp. 17–21.

[13] M. Rodriguez-Damian, E. Cernadas, A. Formella, M. Fernandez-Delgado, and P. D. Sa-Otero, "Automatic detection and classification of grains of pollen based on shape and texture," IEEE Trans. on Systems, Man, and Cybernetics, Applications and Reviews, vol. 36, pp. 531–542, July 2006.

[14] O. Ronneberger, E. Schultz, and H. Burkhardt, "Automated pollen recognition using 3d volume images from fluorescence microscopy," Aerobiologia, vol. 18, no. 2, pp. 107–115, 2002.

[15] M. Rodriguez-Damian, E. Cernadas, A. Formella, and R. Sa-Otero, "Pollen classification using brightnessbased and shape-based descriptors," in International Conference on Pattern Recognition, vol. 2, Aug 2004, pp. 212–215 Vol.2.

[16] Y.-S. Moon, Y.-M. Tai, J. H. Cha, and S.-H. Lee, "A simple ghost-free exposure fusion for embedded hdr imaging," in International Conference on Consumer Electronics (ICCE), Jan 2012, pp. 9–10.

[17] Salem, Mohammed Abdel-Megeed Mohammed & Atef, A & Salah, A & Shams, Marwa. (2018). Recent survey on medical image segmentation. 10.4018/978-1-5225-5204-8.ch006.

[18] Salem, Mohammed Abdel-Megeed Mohammed & Meffert, Beate. (2009). Resolution mosaic EM algorithm for medical image segmentation. Proceedings of the 2009 International Conference on High Performance Computing and Simulation, HPCS 2009. 208 - 215. 10.1109/HPCSIM.2009.5192800.

[19] Shafaey, Mayar & Salem, Mohammed Abdel-Megeed Mohammed & Hegazy, Doaa & Roushdy, Mohamed. (2016). Image segmentation and particles classification using texture analysis method. Research on Biomedical Engineering. 32. 10.1590/2446-4740.03015.

[20] Shafaey, Mayar & Salem, Mohammed Abdel-Megeed Mohammed & Hegazy, Doaa & Ismail Rou, Mohammed. (2016). Image Analysis for Particle Size Recognition of Bioprocesses in Liquid Environment. Asian Journal of Applied Sciences. 9. 170-177.10.3923/ajaps.2016.170.177.

[21] P. sung Liao, T. sheng Chen, and P. choo Chung, "A fast algorithm for multilevel thresholding," Journal of Information Science and Engineering, vol. 17, pp. 713–727, 2001.

[22] M. Varma and A. Zisserman, "A statistical approach to texture classification from single images," International Journal of Computer Vision, vol. 62, no. 1–2, pp. 61–81, 2005.

[23] M. B. Bush and C. Weng, "Introducing a new (freeware) tool for palynology," Journal of Biogeography, vol. 34, no. 3, pp. 377–380, 2007.

[24] Y. Zhai and M. Shah, "Visual attention detection in video sequences using spatiotemporal cues," in Proc. of the 14th Annual ACM Inte. Conf. on Multimedia, 2006, pp.815–824.